Linear extrapolation of ultrarelativistic nucleon-nucleon scattering to nucleus-nucleus collisions

Sangyong Jeon* and Joseph Kapusta[†]

School of Physics and Astronomy, University of Minnesota, Minneapolis, Minnesota 55455
(Received 17 March 1997)

We use a Glauber-like approach to describe very energetic nucleus-nucleus collisions as a sequence of binary nucleon-nucleon collisions. No free parameters are needed: All the information comes from simple parametrizations of nucleon-nucleon collision data. Produced mesons are assumed not to interact with each other or with the original baryons. Comparisons are made to published experimental measurements of baryon rapidity and transverse momentum distributions, negative hadron rapidity and transverse momentum distributions, average multiplicities of pions, kaons, hyperons, and antihyperons, and zero degree energy distributions for sulfur-sulfur collisions at 200 GeV/c per nucleon and for lead-lead collisions at 158 GeV/c per nucleon. Good agreement is found except that the number of strange particles produced, especially antihyperons, is too small compared with experiment. We call this model LEXUS: It is a base-line linear extrapolation of ultrarelativistic nucleon-nucleon scattering to heavy ion collisions. [S0556-2813(97)04807-3]

PACS number(s): 25.75.−q, 24.10.Cn, 24.10.Jv

I. INTRODUCTION

The program to study the properties of quark-gluon plasma at high energy density is in high gear [1] with the construction of the Relativistic Heavy Ion Collider (RHIC) at Brookhaven National Laboratory (BNL) well underway and due to be completed in 1999. In this machine counterrotating beams of gold nuclei with an energy of 100 GeV per nucleon will be collided. The Large Hadron Collider (LHC) at CERN will be completed around the year 2005; it will allow for the collision of counterrotating beams of lead nuclei at about 1.5 TeV per nucleon, but will not be dedicated to heavy ion physics as RHIC will be. Since 1986 experiments have been performed at CERN's SPS accelerator with beams of oxygen and sulfur at 200 GeV/c per nucleon and, lately, lead at 158 GeV/c per nucleon, striking fixed targets. In the same time interval similar beams have been available at BNL's AGS accelerator at the lower energies of 10–14.6 GeV per nucleon. It is almost universally accepted that the proper treatment of collisions at RHIC and LHC must involve the quark and gluon degrees of freedom. At the AGS hadronic degrees of freedom probably suffice (but see [2]). The jury is still out concerning collisions at the SPS.

It is oftentimes heard at conferences and workshops that there is a need for a base-line calculation of what one would expect at the above heavy ion accelerators if there were no new physics, that is, a *linear* extrapolation of nucleon-nucleon collisions to nucleus-nucleus collisions. Construction of such a working model is the goal of this paper. Actually it is not so obvious how to make such a linear extrapolation. Nucleon collisions produce mesons, and these mesons can collide with other nucleons and mesons, producing an interesting cascade of hadrons. We do not consider such a cascade as being a linear extrapolation. The collective excitations of such a system are not necessarily trivial; nor is

it a simple matter to compute or measure all the hadronic cross sections needed to keep track of this cascade. Many such models already exist: ARC [3], RQMD [4], VENUS [5], FRITIOF [6], PYTHIA [7], and QGSM [8] being among the most frequently applied to experimental data.

Our interpretation of a linear extrapolation is based on the 40 year old philosophy and work of Glauber [9] and on the 20 year old rows on rows model of Hüfner and Knoll [10] as applied to the now disassembled Bevalac at LBNL (Lawrence Berkeley National Laboratory). Nucleons from each nucleus follow straight line trajectories, making binary collisions with nucleons from the other nucleus. These collisions are as in free space. Inelastic collisions produce mesons; the mesons are not allowed to collide with each other or with any nucleons. The number of binary collisions suffered by any given nucleon depends on the nucleon cross section and on the geometry of the nuclei. The details will be given in later sections. It is important to know that this linear extrapolation model which we refer to as LEXUS, for linear extrapolation of ultrarelativistic scattering, has no free parameters.

We will apply LEXUS to published data on S+S and Pb+Pb collisions at the SPS. (At this time the quantity of Pb+Pb data available to us is not as complete as the S+S data.) We do not attempt to apply LEXUS to AGS energies. Those energies are probably too low to accept the assumption of straightline trajectories as being anywhere near realistic.

It is important to keep in mind that all LEXUS predictions in this paper are absolutely normalized. We have not attempted to tune the results in any sense.

A conclusion of our paper is that a linear extrapolation of nucleon collisions is consistent with S+S and Pb+Pb collisions at the SPS in the sense that it gives a good representation of the baryon rapidity and transverse momentum distributions, the negative hadron rapidity and transverse momentum distributions, the average number of pions, and zero degree energy distributions. However, it predicts only about 80% of the observed number of charged kaons, 50% of

_____

*Electronic address: jeon@nucth1.spa.umn.edu

[†]Electronic address: kapusta@physics.spa.umn.edu

the number of observed neutral kaons and lambdas, and 10% of the number of observed antilambdas, all in reference to central S+S collisions. This may suggest where new physics lies.

In Sec. II we formulate the model and solve for the basic building blocks, the two-particle baryon rapidity distributions. In Sec. III we compute the final, observable baryon rapidity distribution. In Sec. IV we compute the baryon transverse momentum distribution. In Sec. V we compute the average multiplicities of various produced hadrons. In Sec. VI we compute the negative hadron rapidity distribution. In Sec. VII we compute the transverse momentum distribution of negative hadrons. In Sec. VIII we compute the zero degree (calorimeter) energy distribution. Conclusions are drawn in Sec. IX.

II. FORMULATION AND SOLUTION OF THE MODEL

To formulate the model it is convenient to consider a collision between two rows of nucleons. A nucleus-nucleus collision will be constructed from an ensemble of row-row collisions. Refer to the nucleons comprising these rows as projectile and target nucleons. Let $W_{mn}(y_P, y_T)$ represent the two-particle rapidity distribution for the mth projectile nucleon and the nth target nucleon immediately after their collision. The single-particle projectile distribution $W_{mn}^P(y_P)$ is obtained by integrating the two-particle distribution over the unobserved target rapidity. The index mn then refers to the mth projectile nucleon after colliding with n target nucleons:

$$W_{mn}^P(y_P) = \int dy_T W_{mn}(y_P, y_T). \tag{1}$$

Similarly, $W_{mn}^T(y_T)$ is the single-particle target distribution obtained by integrating over the unobserved projectile rapidity. The index mn then refers to the nth target nucleon after colliding with m projectile nucleons. These single-particle distributions are normalized to unity:

$$\int dy_P W_{mn}^P(y_P) = \int dy_T W_{mn}^T(y_T) = 1. \tag{2}$$

As a result of the indistinguishability of nucleons, the outgoing nucleon with the larger rapidity is called a projectile and the other is called a target.

The two-particle distribution W_{mn} is obtained by the collision between the mth projectile nucleon, which has suffered $n-1$ previous collisions, with the nth target nucleon, which has suffered $m-1$ previous collisions:

$$W_{mn}(y_P, y_T) = \int dy_P' dy_T' W_{mn-1}^P(y_P') W_{m-1n}^T(y_T')$$
$$\times K(y_P' + y_T' \rightarrow y_P + y_T). \tag{3}$$

Here we assume that the process is Markovian with kernel K. This is not a necessary assumption and could be relaxed. Doing so would result in a correlated cascade. However, it would require experimental information on the correlation between the two outgoing baryons which is generally not available.

A basic input is the kernel K which must be taken from experiments on nucleon-nucleon collisions. To that end consider a nucleon-nucleon collision in the laboratory frame of reference so that the initial single-particle distributions are

$$W_{10}^P(y_P') = \delta(y_P' - y_0),$$
$$W_{01}^T(y_T') = \delta(y_T'), \tag{4}$$

where y_0 is the beam rapidity. Substitution into the evolution equation gives

$$W_{11}(y_P, y_T) = K(y_0 + 0 \rightarrow y_P + y_T). \tag{5}$$

Experiments do not measure the correlated two-nucleon distribution over all phase space; they only measure the single-particle distribution:

$$\frac{dN}{dy}(y) = W_{11}^P(y) + W_{11}^T(y). \tag{6}$$

Here the projectile contribution is

$$W_{11}^P(y_P) = \int dy_T W_{11}(y_P, y_T) \tag{7}$$

and similarly for the target contribution.

It has long been known that, to good approximation, the distribution of outgoing nucleons in a high-energy nucleon-nucleon collision is flat in longitudinal momentum or a hyperbolic cosine (symmetric about the c.m.) in rapidity [11,12]. This knowledge does not uniquely determine the two-particle kernel K but, with the additional, sensible, requirements that the projectile distribution be forward peaked and that the simplest mathematical representation be used consistent with the data, leads to the parametrization

$$K(y_P' + y_T' \rightarrow y_P + y_T) = \lambda \frac{\cosh(y_P - y_T')}{\sinh(y_P' - y_T')} \frac{\cosh(y_P' - y_T)}{\sinh(y_P' - y_T')}$$
$$+ (1 - \lambda) \delta(y_P - y_P') \delta(y_T - y_T'). \tag{8}$$

It is convenient for later use to define

$$Q(a, b, c) = \lambda \frac{\cosh a}{\sinh b} + (1 - \lambda) \delta(c). \tag{9}$$

Then the distribution of outgoing projectile nucleons is

$$W_{11}^P(y) = Q(y, y_0, y_0 - y) = \lambda \frac{\cosh y}{\sinh y_0} + (1 - \lambda) \delta(y_0 - y). \tag{10}$$

This is the same distribution [13] as used in the evolution model proposed by Hwa [14] to describe proton stopping in high-energy proton-nucleus scattering and solved and applied to data by Csernai and one of the authors [15]. The distribution is normalized to unity. The parameter λ is the fraction of nucleon-nucleon scatterings that result in a hard collision and $1 - \lambda$ is the fraction that are diffractive or elastic. A recent compilation of data on $p + p \rightarrow p + X$ in the momentum range 12–400 GeV/c leads to $\lambda = 0.6$ [16]. These data and the fit are shown in Fig. 1. Unless otherwise stated
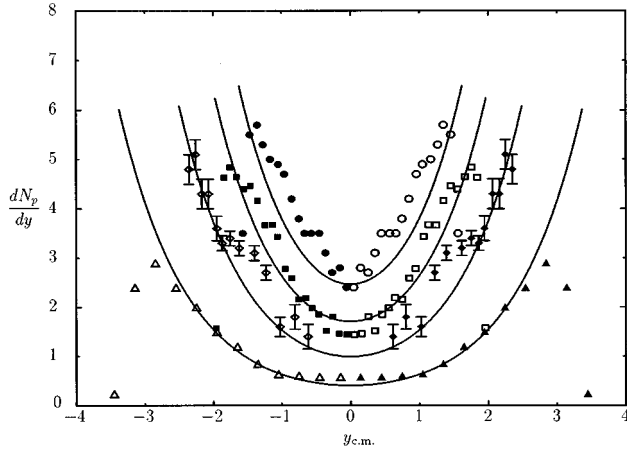
FIG. 1. Proton rapidity distribution in $p+p \rightarrow p+X$ in the center-of-mass frame. From the top: $p_{lab}=12$, 24, 69, and 400 GeV/c. The solid symbols indicate experimentally measured data points and the open symbols are the reflected ones. The solid lines are $dN/dy = \lambda \cosh(y)/\sinh(y_0/2)$ with corresponding maximum rapidity y_0. The data were assembled in Ref. [16].

this is the numerical value used in the rest of the paper. Physical observables turn out to be rather insensitive to small (± 0.1) variations in λ. There is a small rollover in the data near the projectile and target rapidities which is not represented by the parametrization. This has to do with precisely how one separates hard inelastic and diffractive collisions. Our results are only as good as the input parametrizations; in the future it might be worthwhile to treat these components on a finer level.

There is an obvious and useful symmetry between the single-particle projectile and target distributions:

$$W_{mn}^P(y) = W_{nm}^T(y_0 - y). \qquad (11)$$

These distributions are not independent. In the present formulation of the model only single-particle observables may be reliably computed. Hence we only need to compute the $W_{mn}^P(y)$. For this we need an evolution equation. It is obtained by integrating Eq. (3) over the target rapidity and using Eq. (8) for the kernel:

$$W_{mn}^P(y) = \int dy_P dy_T W_{mn-1}^P(y_P) W_{nm-1}^P(y_0 - y_T)$$
$$\times Q(y - y_T, y_P - y_T, y - y_P). \qquad (12)$$

It only remains to solve this Boltzmann-like equation. This can be accomplished by starting with the initial distribution, Eq. (4), and then iterating over all m and n.

A closed form expression can be given for the first nucleon in the row undergoing an arbitrary number of collisions [15]:

$$W_{1n}^P(y) = \frac{\cosh y}{\sinh y_0} \sum_{k=1}^{n} \binom{n}{k} \frac{\lambda^k (1-\lambda)^{n-k}}{(k-1)!} \left[\ln\left(\frac{\sinh y_0}{\sinh y} \right) \right]^{k-1}$$
$$+ (1-\lambda)^n \delta(y_0 - y). \qquad (13)$$

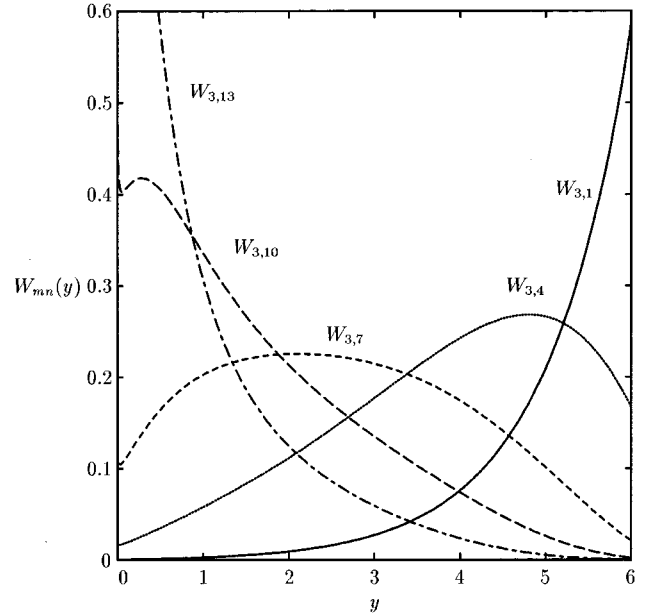Unfortunately we were not able to find a closed expression

FIG. 2. Graphs of $W_{3n}(y)$ for $n=\{1,4,7,10,13\}$.

for arbitrary mn, and so we solved the equations numerically for m and n up to and including 14. The solutions have the form

$$W_{mn}^P(y) = \overline{W}_{mn}^P(y) + (1-\lambda)^n \delta(y_0 - y), \qquad (14)$$

where $\overline{W}$ is a continuous function albeit with logarithmic singularities at $y=0$ and $y=y_0$. These very soft singularities are a consequence of the explicit function Q chosen above. When comparing with experiment it should be remembered to smooth these by the experimental resolution of the detectors. See also Fig. 1 and the previous discussion. We have constructed numerical tables of $\overline{W}$. These may be obtained from the web site of one of the authors [17]. Some representative examples are plotted in Fig. 2.

III. BARYON RAPIDITY DISTRIBUTION

In this section we will apply the most obvious output of the model, the baryon rapidity distribution, to the available experimental data on nucleus-nucleus collisions. But first we must describe how to make a nucleus-nucleus collision out of row-on-row collisions. This is standard material for any Glauber-like model, and so we shall go over it without too much discussion.

Consider a collision between a projectile nucleus and a target nucleus with an impact parameter **b**. We can think of this approximately as a sum of independent collisions between rows of nucleons as illustrated in Fig. 3. Two rows will collide when the transverse position $\mathbf{s}_P$ of the projectile row relative to the projectile nucleus' center of mass and the transverse position $\mathbf{s}_T$ of the target row relative to the target nucleus' center of mass are related by $\mathbf{s}_T = \mathbf{b} + \mathbf{s}_P$. The average numbers of nucleons in each row, with cross sectional area equal to the nucleon-nucleon cross section, are
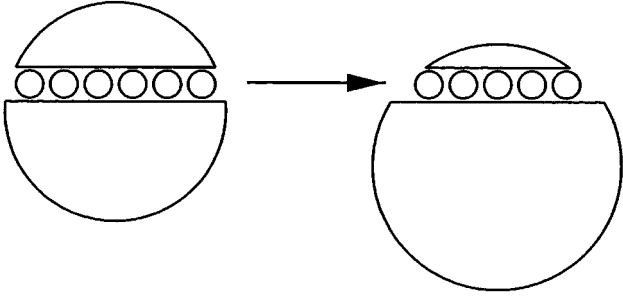
FIG. 3. A schematic view of a row-on-row collision.

$$\nu_P(\mathbf{s}_P) = \sigma_{NN} \int dz \rho_P(\mathbf{s}_P, z),$$

$$\nu_T(\mathbf{s}_T) = \sigma_{NN} \int dz \rho_T(\mathbf{s}_T, z), \qquad (15)$$

where ρ is the baryon density and z is the longitudinal coordinate. Let $\mathcal{P}_{\overline{m}}^P(\mathbf{s}_P)$ and $\mathcal{P}_{\overline{n}}^T(\mathbf{s}_T)$ denote the probability of having $\overline{m}$ and $\overline{n}$ nucleons in the projectile and target rows, respectively, at the given impact parameter. We defer the actual choice of these probabilities.

There will be fluctuations in the number of nucleons in each row. Similarly, there will be fluctuations in the number of collisions suffered by any given nucleon in a row. Taking these into account, results in the contribution of the projectile nucleons to the final baryon rapidity distribution as follows:

$$\frac{dN_P}{dy}(y, \mathbf{b}) = \sum_{m=1}^{A_P} \sum_{\overline{m}=1}^{\overline{m}} \sum_{n=0}^{A_T} W_{mn}^P(y) \int \frac{d^2 s_P}{\sigma_{NN}} \mathcal{P}_{\overline{n}}^T(\mathbf{s}_T) \mathcal{P}_{\overline{m}}^P(\mathbf{s}_P). \qquad (16)$$

There is an analogous expression for the target contribution. The total rapidity distribution at the fixed impact parameter is the sum of the projectile and target contributions.

Now the choice of the $\mathcal{P}$'s must be made. One candidate is a Poisson distribution. Its disadvantage is twofold: It overestimates the magnitude of the fluctuations (they are unlimited in a Poisson but are limited in reality by the number of available nucleons) and it would require knowledge of the W_{mn}^P for arbitrarily large values of m and n, which is computationally infeasible. A natural alternative is a binomial, but with what maximum value? It is physically unreasonable to allow all nucleons in a nucleus to fluctuate into one row. The maximum average value of the nucleons in a given row is about 10 in a large nucleus. We have chosen the maximum value $N_{\max}$ to be 14. Varying this number by 1 or 2 does not change any distribution by more than a percent. Explicitly we have chosen

$$\mathcal{P}_{\overline{m}}^P(\mathbf{s}_P) = \binom{N_{\max}}{\overline{m}} \left[\frac{\nu_P(\mathbf{s}_P)}{N_{\max}} \right]^{\overline{m}} \left[1 - \frac{\nu_P(\mathbf{s}_P)}{N_{\max}} \right]^{N_{\max}-\overline{m}}$$

$$\times \Theta(N_{\max} - \overline{m}). \qquad (17)$$

Here Θ is the step function. For the nucleon-nucleon cross section we use a constant value of 4 fm^2 which is appropriate for beam energies ranging from tens to hundreds of GeV.

For the nuclear density distribution in lead we use a Woods-Saxon function

$$\rho(r) = \frac{\rho_0}{1 + \exp[(r-b)/a]}, \qquad (18)$$

with parameters $a = 0.546$ fm and $b = 6.62$ fm. Normalization to $A = 208$ fixes $\rho_0 = 0.1604$ fm^{-3}. For sulfur we use a three-parameter Gaussian [18]

$$\rho(r) = \frac{\rho_0(1 + wr^2/b^2)}{1 + \exp[(r^2 - b^2)/a^2]}, \qquad (19)$$

with parameters $w = 0.160$, $a = 2.191$ fm, and $b = 2.54$ fm. Normalization to $A = 32$ fixes $\rho_0 = 0.226$ fm^{-3}.

To compare with experimental measurements we must know the trigger conditions; that is, we must know with what probability any particular impact parameter is accepted by the detector. Such a trigger can best be accommodated by an event generator, for then the output of the theory can be sent through the experimental filter. Since our model is not an event generator, at least in its present form, we can only attempt to simulate the trigger as best we can. The procedure we shall use is to make a sharp impact parameter cutoff. The total nucleus-nucleus cross section may be computed following Karol [19]:

$$\sigma_{A_P A_T}^{\text{tot}} = \int d^2 b \{ 1 - \exp[-f(\mathbf{b})] \}. \qquad (20)$$

Here f is the geometrical overlap function of the two nuclei:

$$f(\mathbf{b}) = \int \frac{d^2 s_P}{\sigma_{NN}} \nu_P(\mathbf{s}_P) \nu_T(\mathbf{s}_T). \qquad (21)$$

If only those nucleus-nucleus collisions are accepted with an impact parameter less than or equal to b_{cut}, then the corresponding cross section is

$$\sigma_{A_P A_T}(b_{\text{cut}}) = \int d^2 b \{ 1 - \exp[-f(\mathbf{b})] \} \Theta(b_{\text{cut}} - b). \qquad (22)$$

Clearly

$$\sigma_{A_P A_T}^{\text{tot}} = \lim_{b_{\text{cut}} \to \infty} \sigma_{A_P A_T}(b_{\text{cut}}). \qquad (23)$$

The impact parameter cutoff can be adjusted to reproduce a given centrality cut. For example, if only the 6% ''most central'' collisions are accepted, then b_{cut} is adjusted such that $\sigma_{A_P A_T}(b_{\text{cut}}) = 0.06 \sigma_{A_P A_T}^{\text{tot}}$.

Now we compare with experiment. Figure 4 shows the proton rapidity distribution measured by NA35 [20] for the 2% most central collisions of S+S at a beam energy of 200 GeV/c per nucleon. The solid symbols are the actual measurements and the open symbols are those obtained by reflection about midrapidity. Except possibly for the nuclear fragmentation regions, that is, within ± 1 unit of rapidity of beam and target, the data are represented very well by LEXUS.

The first measurements of the proton rapidity distribution in Pb+Pb collisions at 158 GeV/c per nucleon have just
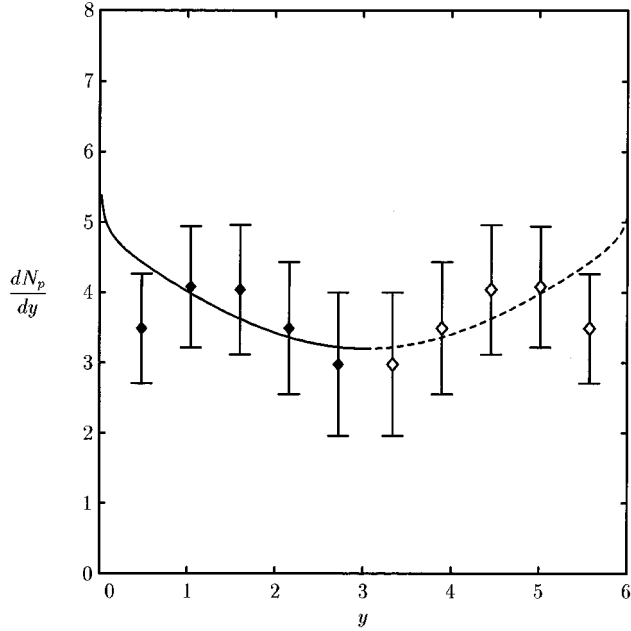
FIG. 4. Proton rapidity distribution for a S+S collision at 200 GeV/c with a centrality of 2%. The solid line represents our calculation. Solid diamonds are data from NA35. Open diamonds and the dashed line are the reflection of the left half.

recently been published by NA44 [21]. They are shown in Fig. 5 and represent the 6.4% most central collisions. The systematic plus statistical uncertainties together are very large, and there are only two measured points. To compare with the proton distributions in Pb+Pb we should point out an uncertainty in our current application of LEXUS. We
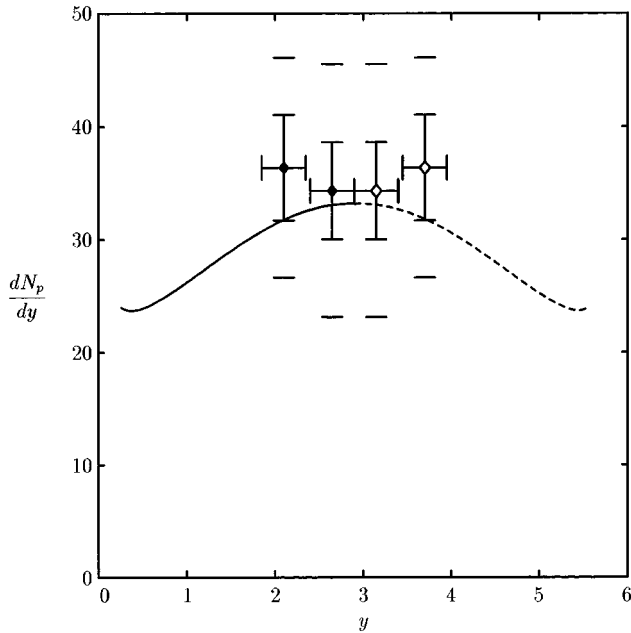

FIG. 5. Proton rapidity distribution for a Pb+Pb collision at 158 GeV/c with a centrality of 6.4%. The solid line is our result. The data points from NA44 are marked by solid diamonds. The open diamonds and the dashed lines are the reflection of the left half. Error bars on the NA44 data represent statistical errors; the limiting short bars represent systematic errors.
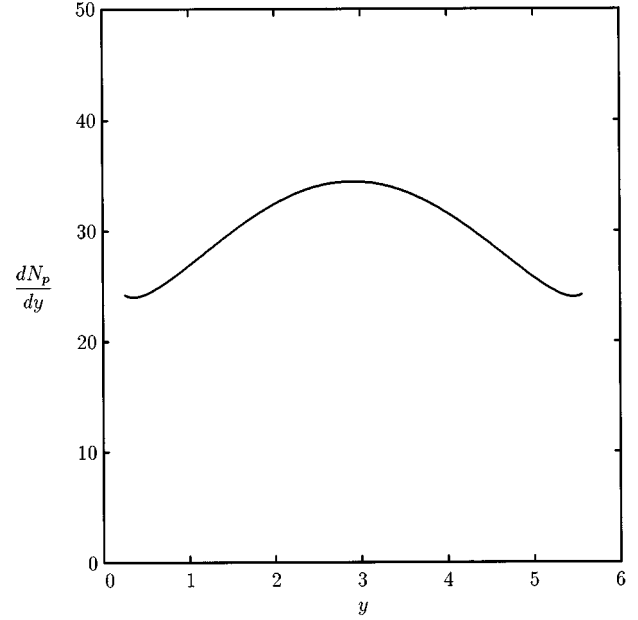

FIG. 6. Proton rapidity distribution for a Pb+Pb collision at 158 GeV/c with 5% centrality.

have not distinguished between outgoing protons and neutrons but have only counted baryons. For collisions of charge asymmetric nuclei at high energy it is reasonable to expect that nearly 1/2 of the outgoing baryons will be protons due to the preference to convert more neutrons into protons than vice versa. This simply follows from phase space and entropy. Accepting that, the LEXUS predictions are in very good agreement with the data.

So far NA49 has not published its measurements of the baryon rapidity distribution in Pb+Pb collisions. The prediction of LEXUS is shown in Fig. 6 for a centrality cut of 5%. The baryon rapidity density for Pb+Pb is higher than that for S+S by an order of magnitude.

IV. BARYON TRANSVERSE MOMENTUM DISTRIBUTION

Even though LEXUS assumes straight-line trajectories, it is still possible to get an enhancement of the baryon transverse momentum compared to nucleon-nucleon collisions. Every time a collision occurs the baryons can get a transverse kick. As long as they continue to travel with high velocity this will not negate the assumption of straightline trajectories. The path of the baryon may be thought of as a random walk in transverse momentum-space. The average transverse momentum-squared of a baryon is related to the average number k of collisions it has suffered according to

$$\langle p_T^2 \rangle_k = k \langle p_T^2 \rangle_{NN}, \tag{24}$$

where $\langle p_T^2 \rangle_{NN}$ is the average in a nucleon-nucleon collision. This quantity is approximately beam energy independent for the beam energies of interest to us [22,23]. We will use $\langle p_T^2 \rangle_{NN} = 0.282$ (GeV/c)^2.

We will assume that the rapidity and transverse momentum distributions factorize in the elementary nucleon-nucleon collisions, which is close to fact except near the

edges of phase space. The transverse momentum distribution is well represented by the thermal form

$$\frac{dN}{p_T dp_T} = \mathcal{N}_1 m_T K_1(m_T/T_1),\qquad (25)$$

where $m_T = \sqrt{m_N^2 + p_T^2}$ is the proton transverse mass and $\mathcal{N}_1$ normalizes the distribution to one. Taking $\langle p_T^2 \rangle_{NN} = 0.282$ $(\text{GeV}/c)^2$ converts into $T_1 = 113$ MeV. After suffering k collisions the baryon transverse momentum distribution becomes broader as reflected in a higher temperature T_k [24] which is determined by

$$\mathcal{N}_k \int_0^\infty dp_T p_T^3 m_T K_1(m_T/T_k) = k\langle p_T^2 \rangle_{NN}.\qquad (26)$$

The transverse momentum distribution of projectile baryons can now be computed by averaging over the number of collisions. For $y \neq y_0$, $p_T \neq 0$ it is

$$\frac{d^2 N^P}{p_T dp_T dy} = \sum_{m=1}^{A_P} \sum_{\bar{m}=1}^{\bar{m}} \sum_{n=1}^{A_T} \frac{\overline{W}_{mn}^P(y)}{1-(1-\lambda)^n} \sum_{k=1}^{n} \binom{n}{k} \lambda^k$$

$$\times (1-\lambda)^{n-k} \mathcal{N}_k m_T K_1(m_T/T_k) \int \frac{d^2 b}{\sigma_{A_P A_T}(b_{\text{cut}})}$$

$$\times \Theta(b_{\text{cut}} - b) \int \frac{d^2 s_P}{\sigma_{NN}} \mathcal{P}_n^T(\mathbf{s}_T) \mathcal{P}_{\bar{m}}^P(\mathbf{s}_P).\qquad (27)$$

The reason for the sum over k at fixed n is that the probability of any given scattering to be considered hard is λ, which is binomially distributed. The $k=0$ term just results in $p_T = 0$. There is an analogous expression for target nucleons.

Now we compare with experiment. The transverse momentum distribution in the 2% most central S+S collisions at 200 GeV/c per nucleon has been measured by NA35 [20]. The data span the rapidity range $0.2 < y < 3.0$ and are shown in Fig. 7. The shape and the absolute normalization are in very good agreement with the results of LEXUS.

The transverse mass distribution for protons from the 6.4% most central Pb+Pb collisions at 158 GeV/c per nucleon have been measured by NA44 [21]. The measurements were performed at $y = 2.10$ and at $y = 2.65$. They are shown in comparison with LEXUS in Fig. 8. The higher rapidity data are again in very good agreement with LEXUS; the lower rapidity data are in less good agreement. The most likely explanation is that we have assumed that elastically or diffractively scattered nucleons acquire zero transverse momentum. Allowing for it would increase the distribution at small p_T nearer the projectile and target rapidities. This is a topic for future investigation.

V. AVERAGE MULTIPLICITIES OF PRODUCED HADRONS

The production of secondary hadrons, such as pions and kaons, or the conversion of the incident nucleons to hyperons, carries additional information about the collision dynamics, in particular the entropy. In LEXUS we assume that mesons are created in the collisions of the cascading baryons as in free space. Once created, the mesons are assumed to
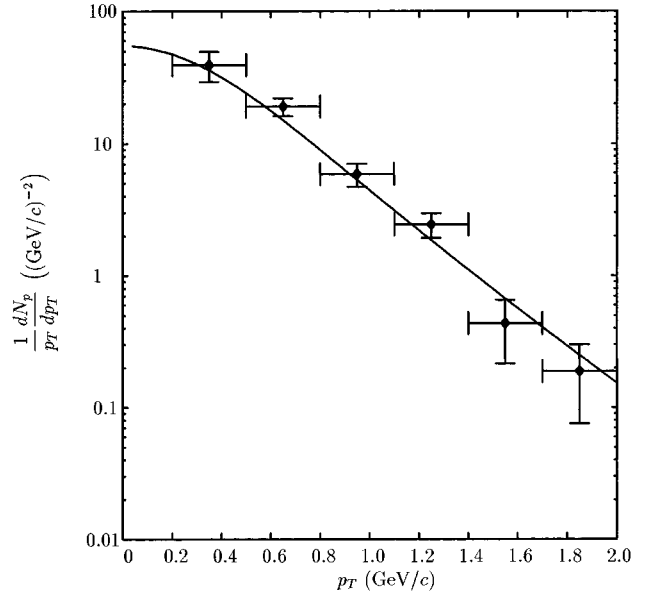

FIG. 7. Proton transverse momentum distribution for a S+S collision at 200 GeV/c with a centrality of 2%. The solid line represents our calculation. Data are from NA35. Rapidity range is $0.2 < y < 3.0$.

freely disperse: They no longer participate in the nuclear collision. The incident nucleons may very well change their character as they cascade: Protons may convert to neutrons and vice versa, or they may be excited into various Δ, N^*, or hyperon states. In this section we will compute the average multiplicities of charged hadrons h^-; kaons K^+, K^-, and K_S^0; and hyperons Λ and $\bar{\Lambda}$. We could compute the full multiplicity distributions, but in this paper we are content to get the average multiplicities.
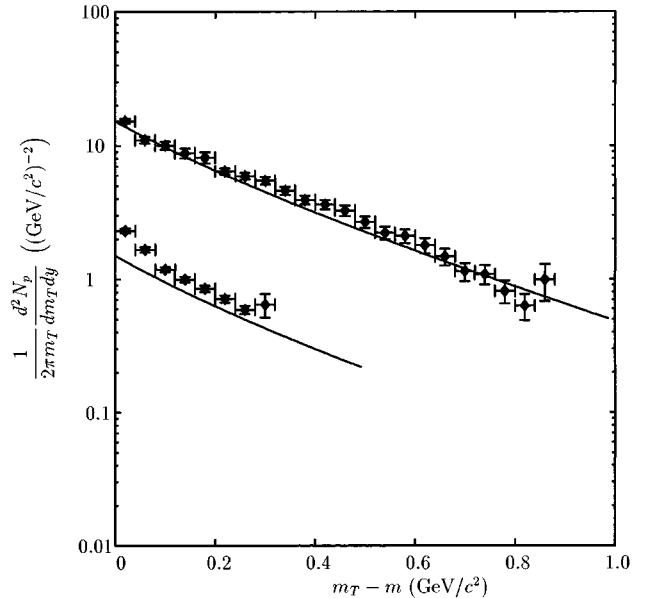

FIG. 8. Proton transverse momentum distribution for a Pb+Pb collision at 158 GeV/c with a centrality of 6.4%. Solid diamonds are NA44 data and the solid curve is our result. The upper curve is for $y = 2.65$. The lower curve is for $y = 2.10$ scaled by a factor of 1/10.

Let $\langle X(s) \rangle_{NN}$ represent the average number of mesons of type X produced in a nucleon-nucleon collision at center-of-mass energy $\sqrt{s}$. The average number of such mesons produced in a collision between the mth projectile nucleon and the nth target nucleon is

$$\langle X_{mn} \rangle = \lambda \int dy_P dy_T W^P_{mn-1}(y_P) W^T_{m-1n}(y_T)$$

$$\times \langle X(y_P - y_T) \rangle_{NN}, \qquad (28)$$

where $\sqrt{s} = 2m_N \cosh[(y_P - y_T)/2]$. The total number produced in a given row-row collision is obtained by summing over all nucleon-nucleon collisions:

$$\langle X(\mathbf{s}_P, \mathbf{s}_T) \rangle = \sum_{m=1}^{A_P} \sum_{n=1}^{A_T} \mathcal{P}^T_n(\mathbf{s}_T) \mathcal{P}^P_m(\mathbf{s}_P) \sum_{m=1}^{\bar{m}} \sum_{n=1}^{\bar{n}} \langle X_{mn} \rangle. \qquad (29)$$

Finally we need to sum over all rows and over all allowed impact parameters:

$$\langle X(b < b_{\mathrm{cut}}) \rangle = \int \frac{d^2 b}{\sigma_{A_P A_T}(b_{\mathrm{cut}})} \Theta(b_{\mathrm{cut}} - b)$$

$$\times \int \frac{d^2 s_P}{\sigma_{NN}} \langle X(\mathbf{s}_P, \mathbf{s}_T) \rangle. \qquad (30)$$

This can be written as a trace over the product of two matrices.

Let us first consider the production of negatively charged hadrons. Gaździcki has shown [25] that the average multiplicity of charged hadrons in isospin averaged nucleon-nucleon collisions for laboratory momenta ranging from 2 to 400 GeV/c is fit to within about 6% by the simple parametrization

$$\langle h^- \rangle_{NN} = 0.784 F_{NN\pi}(s), \qquad (31)$$

where $F_{NN\pi}$ is the Fermi variable modified for the pion production threshold,

$$F_{NN\pi}(s) = \frac{(\sqrt{s} - 2m_N - m_\pi)^{3/4}}{s^{1/8}}, \qquad (32)$$

and where $\sqrt{s}$ is given in GeV. There are two caveats to using this parametrization in LEXUS. The first is that for light nuclei such as oxygen or sulfur the isospin averaging is alright, but for heavier nuclei such as gold or lead it is not. However, after one or two collisions protons are more likely to transform into neutrons than vice versa because of phase space or entropy. Then isospin averaging becomes a better approximation. The second is that occasionally a nucleon can convert into a hyperon. There is essentially no experimental information on the charged hadron multiplicity in a hyperon-nucleon collision, for good reason. Therefore, for lack of any other information, we shall continue to use Gaździcki's parametrization.

There is somewhat less experimental information on the multiplicity of kaons produced in nucleon-nucleon collisions. These data have been compiled by Gaździcki and Röhrich

TABLE I. Table of the parameters for the fits in Eqs. (33) and (34).

	K^+	K^-	K^0_S	Λ	$\bar{\Lambda}$
a	0.208	0.0190	0.0426	0.0891	0.00203
b	6.92	2.62	4.28	4.03	5.67
c	2.24	2.20	0.794	1.16	2.14

[26] and shown to be rather well-defined functions of the Fermi variable. The parametrizations we shall adopt are

$$\langle K^+ \rangle_{NN} = \frac{a F^2_{NNK^+}}{b + (F_{NNK^+} - c)^2},$$

$$\langle K^- \rangle_{NN} = \frac{a F^3_{NNK^-}}{b + (F_{NNK^-} - c)^2},$$

$$\langle K^0_S \rangle_{NN} = \frac{a F^3_{NNK^0_S}}{b + (F_{NNK^0_S} - c)^2}. \qquad (33)$$

The parameters a, b, c are displayed in Table I.

The experimental data on Λ and $\bar{\Lambda}$ production was also analyzed by Gaździcki and Röhrich. We have constructed the following parametrizations for use in LEXUS:

$$\langle \Lambda \rangle_{NN} = \frac{a F^2_{NN\Lambda}}{b + (F_{NN\Lambda} - c)^2},$$

$$\langle \bar{\Lambda} \rangle_{NN} = \frac{a F^3_{NN\bar{\Lambda}}}{b + (F_{NN\bar{\Lambda}} - c)^2}. \qquad (34)$$

These parameters a, b, c are also listed in Table I.

In all cases above the F_{NNX} are defined as

$$F_{NNX} = \frac{(\sqrt{s} - M_X)^{3/4}}{s^{1/8}}, \qquad (35)$$

where the threshold energies are $M_X = M_N + M_\Lambda + M_{K^+}$ for $X = \Lambda$, K^+, and K^0_S; $M_X = 2M_N + M_{K^+} + M_{K^-}$ for K^-; and $M_X = 2M_N + 2M_\Lambda$ for $\bar{\Lambda}$. We have taken into account the uncertainties in the production cross sections in the elementary nucleon-nucleon collisions as illustrated in Fig. 9 for the Λ hyperon. In addition to making a best fit to the data, upper and lower envelopes are constructed which roughly pass through the upper and lower error bars, respectively. (The parameters for these envelopes are not tabulated here.)

Calculated results for S+S collisions are shown in Table II and compared with measurements of NA35 [27,28] for 2% centrality. The LEXUS results are given for 0%, 2%, and 4% most central collisions based on impact parameter. These represent the variation in computed abundances with small variations in impact parameter away from $b = 0$. The experimental data are based on a definition of centrality as those collisions with the highest value of transverse energy. This does not exactly correspond to a sharp range of impact parameter because of fluctuations. A better comparison would involve impact parameter smearing. That is outside the scope of this paper.
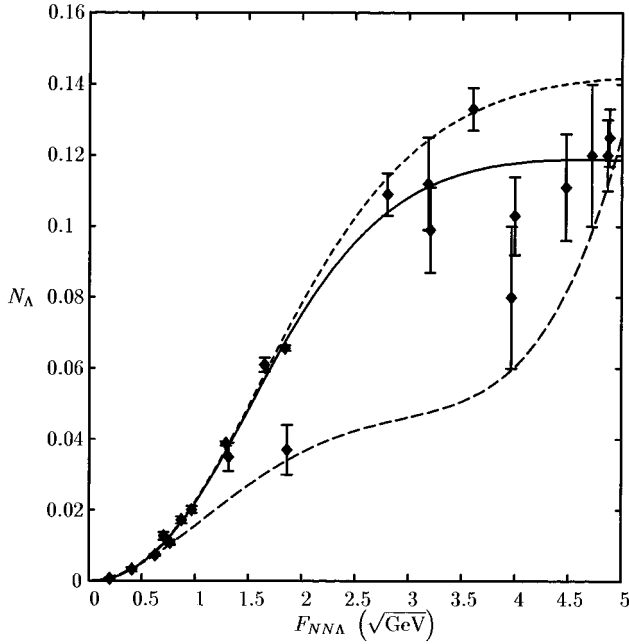
FIG. 9. Data and fits for Λ hyperon production in $p+p$ collisions. The middle line is the weighted fit for the whole data; the upper and the lower lines represent maximum and the minimum envelopes. Experimental data are taken from Ref. [25].

The average number of negatively charged hadrons predicted by LEXUS is in very good agreement with the measurements. The average number of positive or negative kaons obtained from LEXUS is about 80% of that observed. This is a two-standard-deviation effect when account is made of the uncertainty in the production rate in nucleon-nucleon collisions. The number of short-lived neutral kaons is a factor of 2 too small, as is the number of lambdas. The number of antilambdas is nearly an order of magnitude too small compared to experiment. This almost certainly indicates a failure of the model, most likely as a result of the neglect of multiple scattering of produced mesons.

Table III is a prediction of LEXUS for the 5% most central collisions of Pb+Pb at 158 GeV/c per nucleon. No data have yet been published for these abundances.

VI. RAPIDITY DISTRIBUTION OF SECONDARIES

It is important to know where the produced particles emerge in rapidity space. Several types of detectors are able to measure the negative charged hadron rapidity distribution $d\langle h^-\rangle/dy$.

In nucleon-nucleon collisions the charged particle rapidity distribution is approximately Gaussian,

$$\frac{d\langle h^-\rangle_{NN}}{dy} = \frac{\langle h^-\rangle_{NN}}{\sqrt{2\pi}\,\sigma_L(y_{\rm rel})}\exp[-(y-y_{\rm c.m.})^2/2\sigma_L^2(y_{\rm rel})],$$

(36)

with a width given by the Landau model,

$$\sigma_L^2(y_{\rm rel}) = \frac{8}{3}\frac{c_0^2}{1-c_0^4}\ln\left(\frac{\sqrt{s}}{2m_N}\right),$$

(37)

where $y_{\rm rel}=y_P-y_T$ is the relative rapidity of projectile and target and $y_{\rm c.m.}=\frac{1}{2}(y_P+y_T)$ is the rapidity of the center of mass. c_0 is the speed of sound of the produced matter. Not surprisingly $c_0^2\approx1/3$ provides a good fit to nucleon-nucleon data [29]. We have used a very slightly smaller value of 0.32 corresponding to a free gas of massive pions at a temperature of 140–160 MeV. The distinction between 1/3 and 0.32 is irrelevant for the purposes of this paper.

It is straightforward to compute the distribution $d\langle h^-\rangle/dy$ in nucleus-nucleus collisions. All we need to do is replace the quantity $\langle X\rangle_{NN}$ with expression (36) in Eqs. (28)–(30).

The rapidity distribution of h^- has been measured in S+S collisions by NA35 [20]. The results for the 2% most central collisions are shown in Fig. 10. The prediction of LEXUS is also shown and presents a very good representation of the data. Predictions for the 5% most central collisions of Pb+Pb at 158 GeV/c per nucleon are shown in Fig. 11. No data have yet been published.

VII. NEGATIVE HADRON TRANSVERSE MOMENTUM DISTRIBUTION

Mesons are produced when nucleons collide, and since the colliding nucleons are undergoing a random walk in transverse momentum, the mesons will acquire extra transverse momentum too. This is taken into account in the following way.

Suppose that the center-of-mass frame takes discrete steps $\mathbf{v}$ in transverse velocity when baryons undergo hard scattering. The magnitude is fixed but its direction in the transverse plane is random. Then one can show that the average transverse momentum squared of pions produced in a collision between two nucleons which have together undergone i previous scatterings is

$$\langle p_T^2\rangle_i = \langle p_T^2\rangle_\pi + \frac{v^2}{1-v^2}B_i(v^2)\left[\frac{3}{2}\langle p_T^2\rangle_\pi + m_\pi^2\right],$$

(38)

where

TABLE II. The average particle multiplicities in S+S collisions. The NA35 data should be compared against the 2% most central collisions in LEXUS.

	h^-	K^+	K^-	K_S^0	Λ	$\bar{\Lambda}$
NA35	98 ± 3	12.5 ± 0.4	6.9 ± 0.4	10.5 ± 1.7	9.4 ± 1.0	2.2 ± 0.4
LEXUS 0%	106	$9.7\,^{+1.5}_{-2.4}$	$5.7\,^{+0.8}_{-1.4}$	$5.2\,^{+0.2}_{-0.8}$	$4.1\,^{+0.5}_{-2.1}$	$0.29\,^{+0.46}_{-0.17}$
LEXUS 2%	102	$9.4\,^{+1.4}_{-2.3}$	$5.5\,^{+0.8}_{-1.3}$	$5.0\,^{+0.2}_{-0.8}$	$3.9\,^{+0.5}_{-2.0}$	$0.28\,^{+0.44}_{-0.16}$
LEXUS 4%	97.8	$9.0\,^{+1.4}_{-2.2}$	$5.3\,^{+0.8}_{-1.3}$	$4.8\,^{+0.2}_{-0.7}$	$3.8\,^{+0.4}_{-2.0}$	$0.27\,^{+0.43}_{-0.16}$

TABLE III. Predictions for 158 GeV/c Pb+Pb collisions assuming 0 and 5% centrality.

	h^-	K^+	K^-	K_S^0	Λ	$\bar{\Lambda}$
LEXUS 0%	886	$68\,^{+13}_{-16}$	$37\,^{+6}_{-10}$	$35\,^{+0.5}_{-3}$	$33\,^{+3}_{-17}$	$1.6\,^{+2.0}_{-0.9}$
LEXUS 5%	781	$60\,^{+11}_{-14}$	$32\,^{+6}_{-9}$	$31\,^{+0.5}_{-3}$	$29\,^{+3}_{-15}$	$1.4\,^{+1.8}_{-0.8}$

$$B_i(v^2) = \sum_{k=0}^{i-1} \left(\frac{1 + \frac{1}{2}v^2}{1 - v^2} \right)^k. \tag{39}$$

Here $\langle p_T^2 \rangle_\pi$ is the average squared transverse momentum of pions in elementary nucleon-nucleon collisions. Identifying

$$\langle p_T^2 \rangle_{NN} = \frac{4m_N^2 v^2}{1 - v^2}, \tag{40}$$

we obtain $v = 0.272$.

The average value of the pion transverse momentum in elementary nucleon-nucleon collisions varies surprisingly little for beam momenta ranging from 11.6 GeV/c to 195 GeV/c [22]. We shall use $\langle p_T^2 \rangle_\pi = 0.155$ (GeV/c)^2. For pions, too, a good representation of the transverse momentum distribution in nucleon-nucleon collisions is the thermal form (25) with the nucleon mass replaced by the pion mass. This results in a pion temperature in nucleon-nucleon collisions of 133 MeV.

After i previous scatterings of nucleons the pion distribution becomes broader with a temperature T_i determined by

$$\mathcal{N}_i \int_0^\infty dp_T\, p_T^3\, m_T K_1(m_T/T_i) = \langle p_T^2 \rangle_i. \tag{41}$$
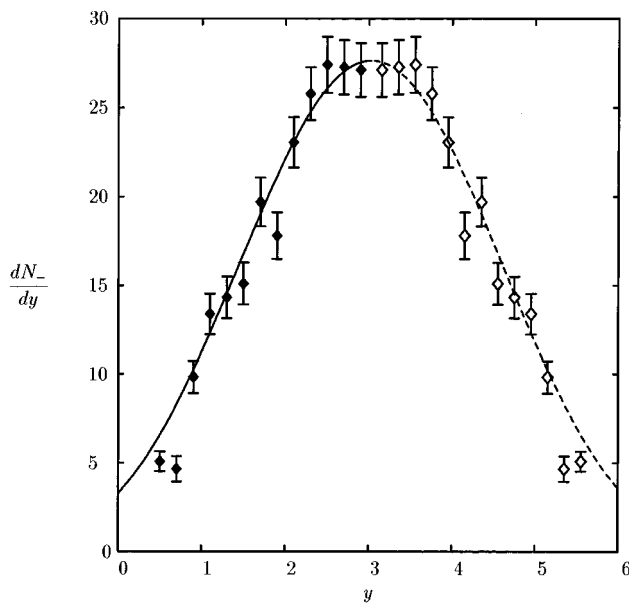

FIG. 10. Rapidity distribution of h^- in 200 GeV/c S+S collisions with a centrality of 2%. The solid line represents our result. Solid diamonds are data from NA35. Open diamonds and the dashed line are the reflection of the left half.
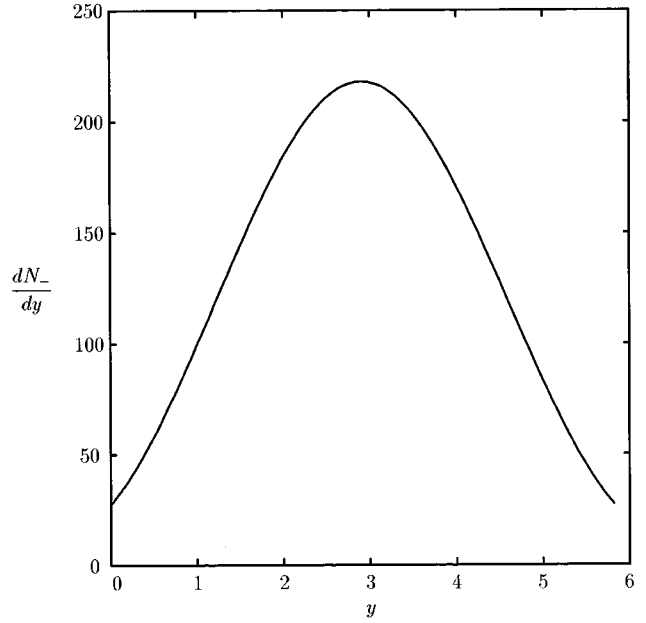

FIG. 11. LEXUS prediction for the rapidity distribution of negatively charged hadrons in 158 GeV/c Pb+Pb collisions with a centrality of 5%.

The full distribution of pions in rapidity and transverse momentum is then computed analogously to the procedure in Sec. V:

$$\frac{d^2 N_{\pi^-}}{p_T dp_T dy} = \sum_{m=1}^{A_P} \sum_{n=1}^{A_T} \mathcal{P}_n^T(\mathbf{s}_T) \mathcal{P}_m^P(\mathbf{s}_P) \sum_{m=1}^{\bar{m}} \sum_{n=1}^{\bar{n}}$$

$$\times \lambda \int dy_P dy_T W_{mn-1}^P(y_P) W_{m-1n}^T(y_T)$$

$$\times \frac{\langle \pi^-(y_{\rm rel}) \rangle_{NN} \exp[-(y - y_{\rm c.m.})^2/2\sigma_L^2(y_{\rm rel})]}{\sqrt{2\pi}\,\sigma_L(y_{\rm rel})}$$

$$\times \mathcal{N}_{n+m-2} m_T K_1(m_T/T_{n+m-2}). \tag{42}$$

A similar analysis can be done for kaons. In this case we use [22] $\langle p_T^2 \rangle_K = 0.290$ (GeV/c)^2. We assume that the sum of the K^- and π^- multiplicities equals the h^- multiplicity.

In Fig. 12 we show the h^- transverse momentum distribution for the 2% most central S+S collisions for the rapidity interval $0.8 < y < 2.0$. The data is from NA35 [20]. In Fig. 13 we show the distribution for the interval $2 < y < 3$. The agreement is acceptable with no surprises. The slight underestimate at very small p_T could be a result of too crude an approximation to the transverse momentum distribution in nucleon-nucleon collisions. It could also be a result of multiple scattering among the produced pions [30]. We do not attempt to compute the distribution for $p_T > 1.5$ GeV/c since the parametrization chosen is not representative of high p_T pion data in nucleon-nucleon collisions.
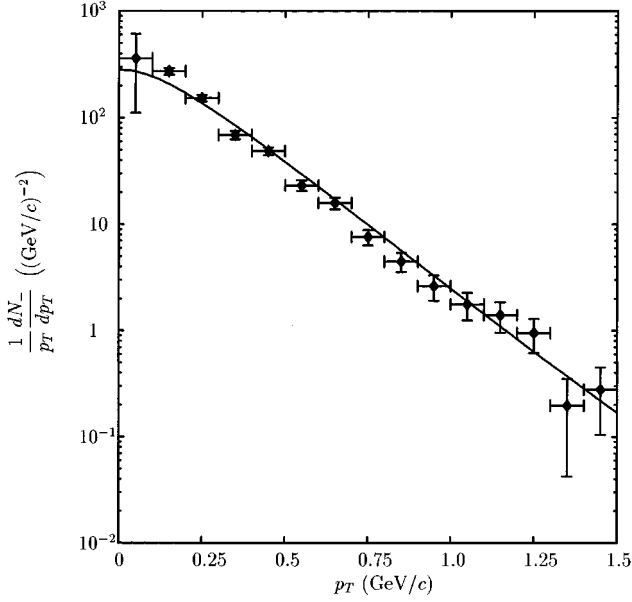
FIG. 12. Negative hadron transverse momentum distribution for a S+S collision at 200 GeV/c with a centrality of 2%. The solid line represents our result and the solid diamonds are NA35 data. Rapidity range is $0.8 < y < 2.0$.

FIG. 13. The same as Fig. 12 but with rapidity range $2.0 < y < 3.0$.

VIII. ZERO DEGREE ENERGY DISTRIBUTION

Many experiments have what is known as a zero degree calorimeter (ZDC) which measures the energy carried by forward going particles in a collision. It is in some sense a measure of impact parameter since any projectile nucleons which participate in the collision get scattered away from the forward direction; to first approximation only spectator nucleons go into the ZDC. There is a monotonic relationship between the average number of spectator nucleons and the impact parameter. The ZDC is oftentimes used as a centrality trigger whereby acceptance of only small energy deposition roughly corresponds to central collisions.

The physics of the ZDC is much more complicated than the basic idea presented above. The ZDC has a very specific response to a given hadron (p, n, π^0, K^-, etc.) with a given laboratory momentum. This response must be accounted for to get an accurate comparison between a model calculation and the data. In this paper we shall make a zero order estimate of the ZDC energy distribution for heavy ion collisions, and then make a first order correction.

In a heavy ion collision a certain number of projectile nucleons will not scatter but will continue along the beam direction without deflection. Knowing this number we can compute the energy deposited in the ZDC (see caveat above). At a given impact parameter the average number of projectile spectator nucleons is

$$N_{\text{spec}}^P(b) = \int \frac{d^2 s_P}{\sigma_{NN}} \sum_{mn} \mathcal{P}_m^P(\mathbf{s}_P) \bar{m} \mathcal{P}_n^T(\mathbf{s}_T)(1-\lambda)^n. \quad (43)$$

Here $\bar{m}$ is the number of projectile nucleons in the row with probability distribution $\mathcal{P}_{\bar{m}}^P$ and $\mathcal{P}_n^T(1-\lambda)^n$ is the probability
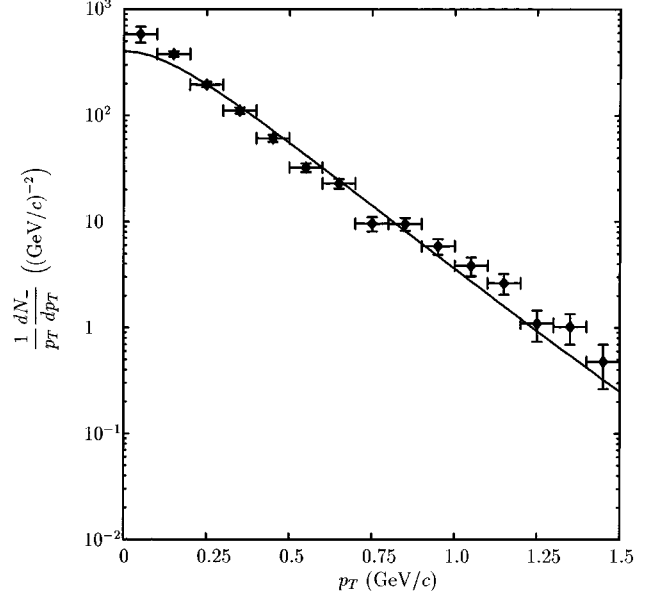
of encountering n target nucleons without suffering any hard scattering. All possibilities are summed over as are all rows. With the probability distribution (17) we get

$$N_{\text{spec}}^P(b) = \int \frac{d^2 s_P}{\sigma_{NN}} \nu_P(\mathbf{s}_P)[1 - \lambda \nu_T(\mathbf{s}_T)/N_{\max}]^{N_{\max}}$$

$$\approx \int \frac{d^2 s_P}{\sigma_{NN}} \nu_P(\mathbf{s}_P) \exp[-\lambda \nu_T(\mathbf{s}_T)]. \quad (44)$$

This has the interpretation of the average number of projectile nucleons in a row times the probability of not making a hard collision with any of the target nucleons, integrated over all rows. When $\lambda \to 0$ or when $b \to \infty$ the average number of spectator projectile nucleons approaches A_P as it should.

There will be fluctuations in the number of spectator nucleons even at fixed impact parameter. The dispersion can be computed in the same way as the average number:

$$D_{\text{spec}}^2(b) = \int \frac{d^2 s_P}{\sigma_{NN}} \sum_{mn} \mathcal{P}_m^P(\mathbf{s}_P) \bar{m} \mathcal{P}_n^T(\mathbf{s}_T)(1-\lambda)^n$$

$$\times [1 - (1-\lambda)^n]$$

$$= \int \frac{d^2 s_P}{\sigma_{NN}} \nu_P(\mathbf{s}_P) \{ [1 - \lambda \nu_T(\mathbf{s}_T)/N_{\max}]^{N_{\max}}$$

$$- [1 - \lambda(2-\lambda)\nu_T(\mathbf{s}_T)/N_{\max}]^{N_{\max}} \}$$

$$\approx \int \frac{d^2 s_P}{\sigma_{NN}} \nu_P(\mathbf{s}_P) \{ \exp[-\lambda \nu_T(\mathbf{s}_T)]$$

$$- \exp[-\lambda(2-\lambda)\nu_T(\mathbf{s}_T)] \}. \quad (45)$$

When $\lambda \to 0$ or when $b \to \infty$ the dispersion goes to zero, consistent with every single one of the projectile nucleons entering the ZDC.
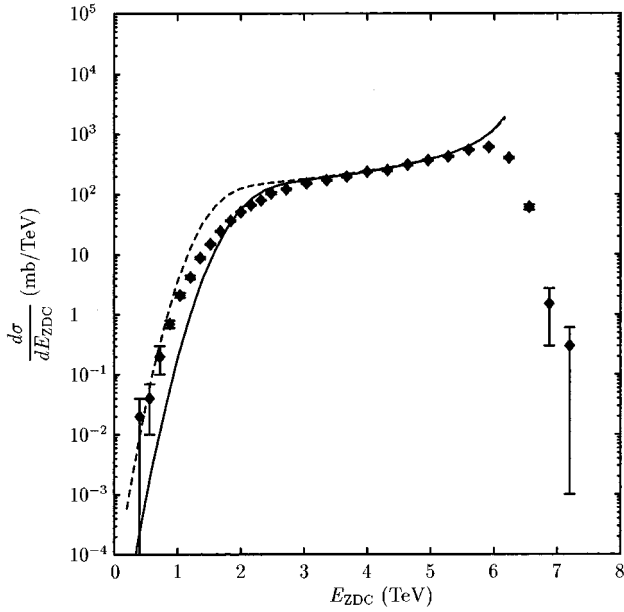
FIG. 14. The zero degree energy distribution for 200 GeV/c S+S collisions. The solid line represents LEXUS with an opening angle of 0.15°. The dashed line represents LEXUS with only the spectator nucleons. Data are from NA35 [31].

FIG. 15. The zero degree energy distribution for 158 GeV/c Pb+Pb collisions. The solid line represents LEXUS with an opening angle of 0.3°. The dashed line represents LEXUS with only the spectator nucleons. Data are from NA49 [32].

We will use the central limit theorem to approximate the conditional probability distribution of the energy carried by projectile spectators into the ZDC at fixed impact parameter by a Gaussian:

$$\frac{d\mathcal{P}}{dE_{\mathrm{ZDC}}}(E_{\mathrm{ZDC}}|b) = \frac{1}{\sqrt{2\pi}D(b)E_{\mathrm{beam}}}\exp\{-[E_{\mathrm{ZDC}}$$
$$-\langle E(b)\rangle]^2/2D^2(b)E_{\mathrm{beam}}^2\}. \qquad (46)$$

Here we have made the identification $\langle E(b)\rangle = E_{\mathrm{beam}}N_{\mathrm{spec}}^P(b)$ and similarly for the dispersion. To get the ZDC energy distribution we integrate over the impact parameter:

$$\frac{d\sigma}{dE_{\mathrm{ZDC}}} = \int d^2b\,\frac{d\mathcal{P}}{dE_{\mathrm{ZDC}}}(E_{\mathrm{ZDC}}|b). \qquad (47)$$

Now we compare with experiment. Data from NA35 for S+S [31] are shown in Fig. 14 as well as the cross section for forward-going nucleons in LEXUS (dashed curve). The central plateau is just about right, as it should be, reflecting the basic geometry of the nuclei. The data go beyond the kinematical limit of 6.4 TeV in a single S+S collision as a result of inefficiencies in the detector. LEXUS predicts too much cross section for forward-going energies of 1–2 TeV.

Data from NA49 for Pb+Pb collisions [32] are shown in Fig. 15. Once again the central plateau is correctly reproduced, but the shoulder at low energy, indicating the most central collisions, is shifted too far left by about 4 TeV. This ZDC is improved over that of NA35 and does not go beyond the kinematic limit of 32.9 TeV.
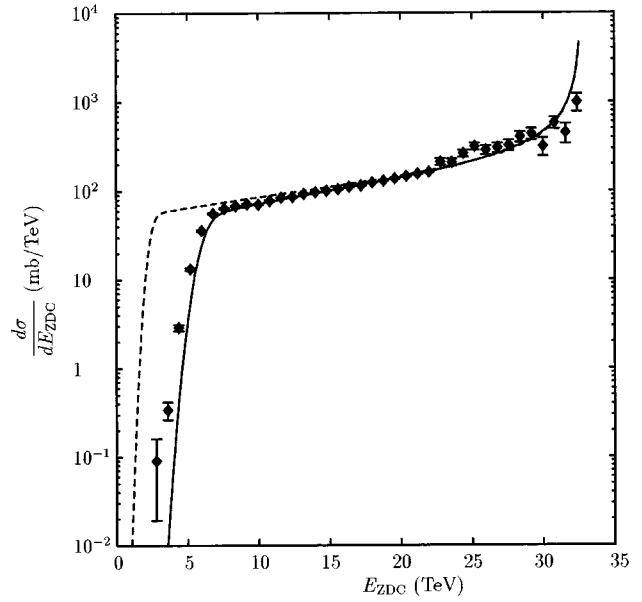
In actual experiments there is a finite opening angle θ_0 for particle acceptance in the ZDC. This is generally a fraction of a degree, in the laboratory frame of course. Some of the hard scattered nucleons, both projectile and target, may emerge with a laboratory angle smaller than this. This effect will tend to increase the energy flow into the ZDC at a fixed impact parameter. The additional energy entering the ZDC is

$$E_{0<\theta<\theta_0}(b) = \int dy\,dp_T(m_T\cosh y - m_N)\frac{d^2N^P}{dp_T dy}(b,p_T,y)$$
$$\times \Theta(\theta_0 - \tan^{-1}(p_T/m_T\sinh y)). \qquad (48)$$

Here $d^2N^P/dp_T dy$ is the same as expression (27) but without the averaging over impact parameter. Then in Eq. (46) we identify $\langle E(b)\rangle = E_{\mathrm{beam}}N_{\mathrm{spec}}^P(b) + E_{0<\theta<\theta_0}(b)$. In addition, the dispersion in the energy entering the ZDC increases and can be estimated by

$$D^2(b) = \int \frac{d^2s_P}{\sigma_{NN}}\sum_{mn}\mathcal{P}_{\bar{m}}(\mathbf{s}_p)\mathcal{P}_n(\mathbf{s}_T)\sum_{m=1}^{\bar{m}}\sigma_{mn}^2. \qquad (49)$$

Here

$$\sigma_{mn}^2 = \int dy\int_0^{p_T^{\max}}dp_T E_K^2\frac{d^2N_{mn}^P}{dp_T dy}(p_T,y)$$
$$- \left(\int dy\int_0^{p_T^{\max}}dp_T E_K\frac{d^2N_{mn}^P}{dp_T dy}(p_T,y)\right)^2$$
$$+ \text{target contribution,} \qquad (50)$$

where $E_K = (m_T \cosh y - m_N)$, $p_T^{\max} = \tan\theta_0 m_T \sinh y$, and

$$\frac{d^2 N_{mn}^P}{p_T dp_T dy}(p_T, y) = \frac{\overline{W}_{mn}^P(y)}{1 - (1-\lambda)^n} \sum_{k=1}^{n} \binom{n}{k} \lambda^k$$

$$\times (1-\lambda)^{n-k} \mathcal{N}_k m_T K_1(m_T/T_k)$$

$$+ (1-\lambda)^n \delta(y - y_0)\delta(p_T). \qquad (51)$$

The target contribution is obtained by simply changing $y \to y_0 - y$.

Now we recompare with experiments. The results of LEXUS with an opening angle of 0.15° is shown in Fig. 14 by the solid curve. The result of allowing some of the scattered nucleons to enter the ZDC is obvious; it reduces the cross section at small forward energies. The results for Pb+Pb with an opening angle of 0.3° are shown in Fig. 15 also with a solid curve. The better agreement for Pb than for S is somewhat mysterious. The opening in the ZDC for both experiments was actually a square, not a circle, with an aperture of 86 μsr. It is quite possible that the simple angle cutoff we have used does not do justice to the complicated workings of these calorimeters. It is also quite possible that our use of a baryon distribution which factorizes in rapidity and transverse momentum in nucleon-nucleon collisions is too crude near the edges of phase space, such as for very forwardgoing nucleons.

IX. CONCLUSION

In this paper we have constructed a means to make a linear extrapolation of nucleon-nucleon collisions to very-high-energy nucleus-nucleus collisions. We call this extrapolation procedure LEXUS. There is no reference to quarks, gluons, strings, Pomerons, or QCD. The treatment is simply based on a sequence of binary nucleon-nucleon collisions as in free space. We know that this treatment cannot be exact as all of our accumulated knowledge of QCD and high-energy physics of the last 25 years can attest. But it is important to do these calculations as a base line against more detailed, but of necessity approximate, treatments based on perturbative and nonperturbative QCD to discover thermodynamic properties of quark-gluon plasma and hadronic matter. What have we learned?

The rapidity and transverse momentum distributions of baryons in central sulfur-sulfur and lead-lead collisions at the SPS seem to be well described by LEXUS. The same can be said for the multiplicity of negatively charged hadrons and their rapidity and transverse momentum distributions. The zero degree energy distribution for lead-lead comes out just about right; for sulfur-sulfur the agreement is less good. This may be due to our rather simple treatment of elastic and diffractive nucleon-nucleon collisions which are more likely to influence the outcome of the collisions between smaller nuclei.

What is not reproduced so well by LEXUS is the abun-

dance of strange particles. Formation of quark-gluon plasma increases the number of strange quarks in the system due to its relatively small mass in comparison to the kaon mass [33]. But it is also possible to increase the number of kaons over that produced in nucleon-nucleon collisions by multiple scattering and attendant pair production of kaons [34]. Most notably the number of antilambdas is too small in LEXUS in comparison to central sulfur-sulfur data by almost an order of magnitude, indicating that there are proportionally many more antistrange quarks in the heavy ion collision than in nucleon collisions [35]. This is interesting physics. It has been discussed several times at Quark Matter conferences [1]. Our calculations confirm it. We anxiously await published data on strangeness in central lead-lead collisions.

There is a preliminary conference report on a forward-backward azimuthal asymmetry in Pb-Pb collisions [36]. This asymmetry is similar to that seen at much lower Bevalac energies. It has been interpreted variously as a collective bounce-off, as if the two nuclei were behaving as fluids, and as the absorption of particles in the cold spectator matter. In either way of thinking the present linear extrapolation of nucleon-nucleon scattering does not take this crosstalk of rows into consideration. It would be challenging to do so [37].

A linear extrapolation like LEXUS is only as good as the data input from nucleon-nucleon collisions. In this paper we have used reasonably accurate yet simple parametrizations of the basic input data. Nevertheless, improvements can be made. For example, our treatment of the elastic and diffractive components of nucleon-nucleon collisions could be represented more accurately but at the cost of significant complication to the solution to the model as described in Sec. II. A better prediction for the baryon momentum distribution near the projectile and target rapidities would likely result, as would a description of the energy deposited in a zero degree calorimeter. Even then, our ability to make a linear extrapolation will be hindered by the lack of experimental measurements of many-particle correlations, such as between the two outgoing baryons in an elementary collision, or the correlation between the rapidities of outgoing baryons with the number of produced mesons. It is unlikely that all the exclusive cross sections for nucleon-nucleon, nucleon-hyperon, and hyperon-hyperon collisions at all the energies of relevance will ever be known experimentally. This is a particular shortcoming if one wants to make a Monte Carlo event generator out of LEXUS. In case of improvements to LEXUS in the future the model described in this paper will be known as version 1.0.

We have not made any comparison to transverse energy distributions as measured by electromagnetic calorimeters. Many such measurements have been made, but it is a challenging task to normalize them in such a way that we can know how much energy each type of hadron (p, n, π^0, K^-, etc.) actually deposits to within a certain accuracy to make a comparison meaningful. This will be the subject of a future application of LEXUS.

Also under study is an application of LEXUS to some very interesting results on the production of J/ψ, photons, and lepton pairs as discussed in recent Quark Matter conferences [1].

Finally, it would be interesting to make LEXUS predictions for RHIC where we certainly anticipate it to fail, lacking a description of hard perturbative QCD [38,39] and the inside-outside cascade effect [40]. The difficulty is that there are no nucleon-nucleon data available at RHIC energy before the turn-on of the accelerator. Nevertheless, a prediction for the baryon rapidity distribution may be considered and is now in progress.

ACKNOWLEDGMENTS

[1] See the proceedings of recent *Quark Matter* conferences: Nucl. Phys. **A566** (1993); **A590** (1995); **A610** (1996).

[2] J. I. Kapusta, A. P. Vischer, and R. Venugopalan, Phys. Rev. C **51**, 901 (1995); J. I. Kapusta and A. P. Vischer, *ibid.* **52**, 2725 (1995).

[3] Y. Pang, T. J. Schlagel, and S. H. Kahana, Phys. Rev. Lett. **68**, 2743 (1992); T. J. Schlagel, Y. Pang, and S. H. Kahana, *ibid.* **69**, 3290 (1992); S. H. Kahana, Y. Pang, T. J. Schlagel, and C. Dover, Phys. Rev. C **47**, R1356 (1993).

[4] H. Sorge, H. Stöcker, and W. Greiner, Ann. Phys. (N.Y.) **192**, 266 (1989); R. Mattiello, H. Sorge, H. Stöcker, and W. Greiner, Phys. Rev. Lett. **63**, 1459 (1989); H. Sorge, A. V. Keitz, R. Mattiello, H. Stöcker, and W. Greiner, Phys. Lett. B **243**, 7 (1990); A. V. Kreitz, L. Winckelmann, A. Jahns, H. Sorge, H. Stöcker, and W. Greiner, *ibid.* **263**, 353 (1991).

[5] K. Werner, Phys. Rep. **232**, 87 (1993).

[6] B. Andersson, G. Gustafson, and B. Nilsson-Almqvist, Nucl. Phys. **B281**, 289 (1987).

[7] H.-U. Bengtsson and T. Sjostrand, Comput. Phys. Commun. **46**, 43 (1987); T. Sjostrand, *ibid.* **82**, 74 (1994).

[8] N. S. Amelin and L. V. Bravina, Yad. Fiz. **51**, 211 (1990) [Sov. J. Phys. **51**, 133 (1990)]; N. S. Amelin, L. V. Bravina, and L. N. Smirnova, *ibid.* **50**, 1705 (1989) [**50**, 1058 (1989)]; **51**, 892 (1990) [**51**, 567 (1990)]; N. S. Amelin, L. V. Bravina, L. I. Sarycheva, and L. N. Smirnova, *ibid.* **51**, 841 (1990) [**51**, 535 (1990)].

[9] R. J. Glauber, in *Lectures in Theoretical Physics*, edited by W. E. Brittin and L. G. Dunham (Interscience, New York, 1959).

[10] J. Hüfner and J. Knoll, Nucl. Phys. **A290**, 460 (1977).

[11] M. A. Abolins *et al.*, Phys. Rev. Lett. **25**, 126 (1970).

[12] J. Whitmore, S. J. Barish, D. C. Colley, and P. F. Schultz, Phys. Rev. D **18**, 3115 (1978).

[13] This reduces to the distribution Q used in [14] and [15] if the nucleon mass is neglected at high momentum.

[14] R. C. Hwa, Phys. Rev. Lett. **52**, 492 (1984).

[15] L. P. Csernai and J. I. Kapusta, Phys. Rev. D **29**, 2664 (1984); *ibid.* **31**, 2795 (1985).

[16] Ole Hansen and F. Videbaek, Phys. Rev. C **52**, 2684 (1995). In this paper the authors look for a scaling behavior of the baryon rapidity distribution in terms of the variable y/y_0 which does not exist.

[17] To be made available after publication of this paper.

[18] H. de Vries, C. W. de Jager, and C. de Vries, At. Data Nucl. Data Tables **36**, 495 (1987).

[19] P. J. Karol, Phys. Rev. C **11**, 1203 (1975).

[20] NA35 Collaboration, J. Bächler *et al.*, Phys. Rev. Lett. **72**, 1419 (1994).

[21] NA44 Collaboration, I. G. Bearden *et al.*, Phys. Lett. B **388**, 431 (1996).

[22] Y. Eisenberg *et al.*, Nucl. Phys. **B154**, 239 (1979).

[23] Much data has been assembled and parametrized in E. E. Zabrodin *et al.*, Phys. Rev. D **52**, 1316 (1995).

[24] By temperature we mean a parameter characterizing a distribution. We make no connection to thermodynamics in this paper.

[25] M. Gaździcki, Z. Phys. C **66**, 659 (1995); M. Gaździcki and D. Röhrich, *ibid.* **65**, 215 (1995).

[26] M. Gaździcki and D. Röhrich, Z. Phys. C **71**, 55 (1996).

[27] NA35 Collaboration, J. Bächler *et al.*, Z. Phys. C **58**, 367 (1994).

[28] NA35 Collaboration, T. Alber *et al.*, Z. Phys. C **64**, 195 (1994).

[29] P. Carruthers and Minh Duong-van, Phys. Rev. D **8**, 859 (1973).

[30] G. M. Welke and G. F. Bertsch, Phys. Rev. C **45**, 1403 (1992); H. W. Barz, G. Bertsch, P. Danielewicz, H. Schulz, and G. M. Welke, Phys. Lett. B **287**, 40 (1992).

[31] NA35 Collaboration, J. Bächler *et al.*, Z. Phys. C **52**, 239 (1991).

[32] NA49 Collaboration, T. Alber *et al.*, Phys. Rev. Lett. **75**, 3814 (1995).

[33] J. Rafelski and B. Müller, Phys. Rev. Lett. **48**, 1066 (1982); **56**, 2334E (1986).

[34] J. Kapusta and A. Mekjian, Phys. Rev. D **33**, 1304 (1986).

[35] P. Koch, B. Müller, and J. Rafelski, Phys. Rep. **142**, 167 (1986).

[36] NA49 Collaboration, T. Wienold *et al.*, Nucl. Phys. **A610**, 76c (1996).

[37] N. S. Amelin *et al.*, Phys. Rev. **67**, 1523 (1991).

[38] K. Geiger, Phys. Rep. **258**, 237 (1995).

[39] X.-N. Wang, Phys. Rep. **280**, 287 (1997).

[40] J. D. Bjorken, Phys. Rev. D **27**, 140 (1983).